Effects of pressure on the ferromagnetic state of the CDW compound $SmNiC_2$

B. Woo, S. Seo, E. Park, J. H. Kim, D. Jang, T. Park
Department of Physics, Sungkyunkwan University, Suwon 440-746, Korea

H. Lee, F. Ronning, J. D. Thompson
Los Alamos National Laboratory, Los Alamos, New Mexico 87545, USA

V. A. Sidorov
Los Alamos National Laboratory, Los Alamos, New Mexico 87545, USA
Institute for High Pressure Physics of Russian Academy of Sciences, RU-142190 Troitsk, Moscow, Russia
Moscow Institute of Physics and Technology, RU-141700 Dolgoprudny, Moscow Region, Russia

Y. S. Kwon
Department of Emerging Materials Science, Daegu Gyeongbuk
Institute of Science and Technology (DGIST), Daegu 711-873, Korea

We report the pressure response of charge-density-wave (CDW) and ferromagnetic (FM) phases of the rare-earth intermetallic $SmNiC_2$ up to 5.5 GPa. The CDW transition temperature (T_{CDW}), which is reflected as a sharp inflection in the electrical resistivity, is almost independent of pressure up to 2.18 GPa but is strongly enhanced at higher pressures, increasing from 155.7 K at 2.2 GPa to 279.3 K at 5.5 GPa. Commensurate with the sharp increase in T_{CDW}, the first-order FM phase transition, which decreases with applied pressure, bifurcates into the upper (T_{M1}) and lower (T_c) phase transitions and the lower transition changes its nature to second order above 2.18 GPa. Enhancement both in the residual resistivity and the Fermi-liquid T^2 coefficient A near 3.8 GPa suggests abundant magnetic quantum fluctuations that arise from the possible presence of a FM quantum critical point.

PACS numbers: 71.27.+a, 68.35.Rh, 71.45.Lr, 75.50.Cc

Low dimensional metallic systems have attracted much interest because of their propensity towards an ordered phase. Density waves are prominent examples in quasi-one-dimensional compounds, where a large anisotropy in the Fermi surface leads to a structural instability accompanied by a periodic lattice distortion[1]. Sensitivity to the Fermi surface topology makes it relatively easy to tune the ordered phases via such external parameters as chemical doping, pressure, and magnetic fields. For the transition-metal dichalcogenide $TiSe_2$, a CDW transition temperature is suppressed with increasing Cu intercalation and is intercepted by a dome of superconductivity centered around a projected critical concentration where the extrapolated T_{CDW} becomes zero.[2] External pressure acts similarly to suppress the CDW phase of $TiSe_2$, inducing superconductivity in the vicinity of a projected CDW critical point.[3] These results both by Cu intercalation and external pressure suggest that correlated electrons spontaneously adjust to a new emergent phase in the vicinity of a quantum critical point.

Rare-earth intermetallic compounds ReNiC$_2$ (Re =La, Ce, Nd, Sm, Gd, Tb, Er) show various ground states of CDWs and magnetism.[4,5] Among the intermetallics, $SmNiC_2$ is unique in that it becomes ferromagnetic, while other members are prone to an antiferromagnetic instability. X-ray scattering studies of $SmNiC_2$ reveal satellite peaks corresponding to an incommensurate wave vector (0.5, 0.52, 0) below 148 K, signaling formation of a charge-density wave.[6] The abrupt disappearance of the satellite peak at the ferromagnetic transition temperature (T_c = 17.4 K) indicates a destruction of the CDW phase and a strong correlation between the FM and CDW phases. First-principles electronic structure calculations find that Fermi-surface nesting is important for the CDW state and weaker nesting in the ferromagnetic phase leads to the destruction of the CDW below T_c (ref. 7). Kim et al. recently estimated that hydrostatic pressure will enhance the CDW because the lattice constant of the Ni chain along the a-axis decreases faster than other axes, thus enhancing the Fermi surface nesting quality.[8] Here, we report the electrical resistivity of $SmNiC_2$ under pressure up to 5.5 GPa. The CDW transition at 151.7 K (=T_{CDW}) is almost independent of pressure up to 2.18 GPa but linearly increases thereafter to 279.4 K at 5.5 GPa. Commensurate with the change in the CDW phase, an additional CDW phase observed at 1.47 GPa and 75 K (=T_{CDW2}) initially increases with pressure, reaches a peak at 2.18 GPa and is suppressed with further increasing pressure. The first-order ferromagnetic transition at 17.4 K that completely replaces the CDW state decreases with pressure and changes its nature to second order above 2.18 GPa, the critical pressure where T_{CDW} sharply increases while the pressure-induced T_{CDW2} starts to decrease. Even though enhancement both in the residual resistivity and the Fermi-liquid T^2 coefficient A near 3.8 GPa suggests abundant magnetic quantum fluctuations, appearance of new magnetic phases at 3.8 and 5.4 GPa hides the possible pres-

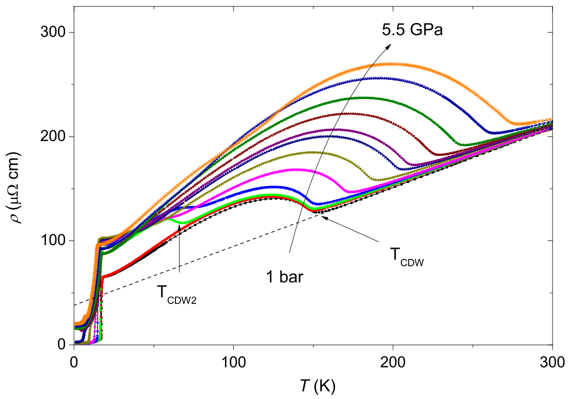

FIG. 1: (Color online) Temperature dependence of the electrical resistivity of $SmNiC_2$ for pressures of 1 bar, 0.87, 1.47, 2.18, 2.72, 3.22, 3.70, 3.86, 4.28, 4.7, 5.14, and 5.5 GPa from the tail to the head of the arrow. T_{CDW} denotes a CDW (charge-density-wave) phase transition temperature, while T_{CDW2} is a pressure-induced CDW transition temperature at a lower temperature, which appears at pressures above 1.47 GPa (green line). The dashed line is a guide to eyes that shows a linear-in-T dependence of the high-temperature resistivity at ambient pressure.

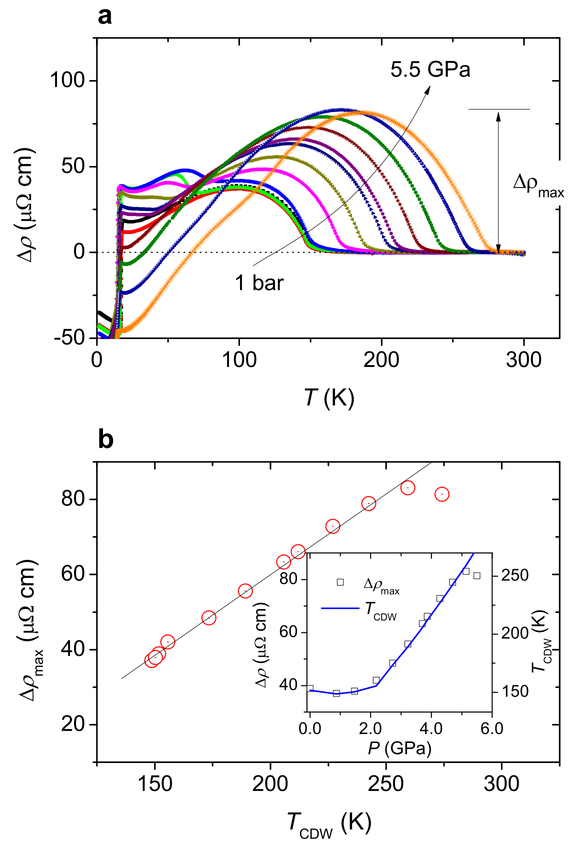

FIG. 2: (Color online) (a) Electrical resistivity difference of $SmNiC_2$ as a function of temperature for 1 bar, 0.87, 1.47, 2.18, 2.72, 3.22, 3.70, 3.86, 4.28, 4.7, 5.14, and 5.5 GPa from the tail to the head of the arrow, where the resistivity difference $\Delta\rho$ is obtained by subtracting the high-T linear behavior: $\Delta\rho = \rho - (a + bT)$. (b) Maximum of the resistivity difference ($\Delta\rho_{max}$) plotted as a function of the CDW transition temperature T_{CDW}. The solid line is a guide to eyes and reflects a linear proportionality between the two parameters. Inset: Pressure dependence of $\Delta\rho_{max}$ (open squares) and T_{CDW} (solid line) is plotted on the left and right ordinates, respectively.

ence of a FM quantum critical point.

$SmNiC_2$ polycrystals were synthesized by arc melting.[9] The constituent elements of Sm, Ni, and C were prepared at a 1.1:1:2 molecular weight ratio because Sm has higher vapor pressure. Polycrystals synthesized in a tetra arc furnace were annealed at 900 °C for 10 days. X-ray powder diffraction showed that they form in a single phase with the $CeNiC_2$-type orthorhombic crystalline structure and with lattice constants $a = 3.7073 Å$, $b = 4.5294 Å$, and $c = 6.0998 Å$. Pressure measurements to 5.5 GPa were performed by using a toroid-type anvil cell with an alumina-epoxy gasket and a glycerol-water mixture as a pressure medium inside the gasket. The superconducting transition temperature of lead was used to determine the pressure in the cell.[10,11] The electrical resistivity of $SmNiC_2$ was measured by a conventional four-probe technique via an LR700 Resistance Bridge from 300 K to 1.2 K in a ^{4}He cryostat.

Figure 1 shows the electrical resistivity ρ of $SmNiC_2$ as a function of temperature under pressure. At ambient pressure, ρ decreases linearly with decreasing temperature and shows an inflection due to a gap opening below the CDW transition temperature T_{CDW} (=151.7 K). With further decreasing temperature, ρ decreases by an order of magnitude due to electrical conduction in ungapped portions of the Fermi surface and the destruction of the CDW gap at the ferromagnetic transition temperature T_c (=17.4 K). The low-temperature resistivity follows a T^2 Landau-Fermi liquid behavior with $\rho_0 = 1.798$ $\mu\Omega$·cm, where the large residual resistivity ratio (RRR=115) indicates high quality of the specimen. The Sommerfeld coefficient γ estimated from the coefficient A (=6.08 × 10^{-4} $\mu\Omega$·cm·K^{-2}) and the Kadowaki-Woods ratio[12] ($R_{KW} = A/\gamma^2 = 1.0 \times 10^{-5}$ $\mu\Omega$·mol^2·cm·K^{-2}·mJ^{-2}) is 7.80 mJ·mol^{-1}·K^{-2}, which is similar to γ (=8 mJ·mol^{-1}·K^{-2}) obtained from specific heat measurements.[9]

Figure 2a depicts the resistivity difference under pressure, $\Delta\rho = \rho - (a + bT)$, where a linear background contribution observed at higher temperatures (see dashed line in Fig. 1 at ambient pressure) is subtracted from ρ of $SmNiC_2$. At 0.87 GPa, as shown in Fig. 2b inset, T_{CDW} decreases to 149.6 K at a depression rate of 2.4 K/GPa and the maximal value in the resistivity difference ($\Delta\rho_{max}$) also decreases. With further increasing pressure, however, T_{CDW} reaches a minimum near 1.47 GPa and increases, showing a linear-in-P dependence at higher pressures with a slope of 15 K/GPa. Figure 2b shows that $\Delta\rho_{max}$ linearly depends on T_{CDW},

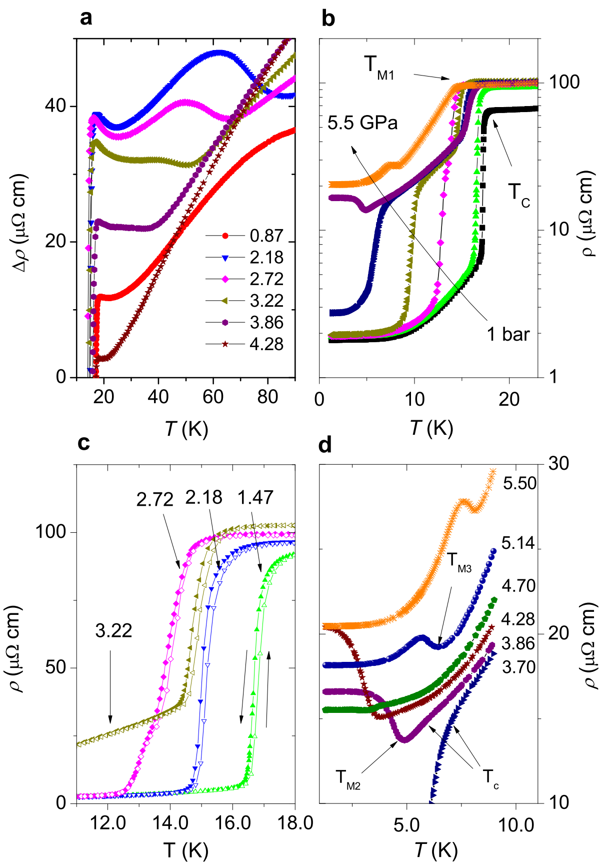

FIG. 3: (Color online) (a) Electrical resistivity difference of $SmNiC_2$ over a limited temperature range to show the pressure-induced CDW phase transition from 0.87 to 4.28 GPa. (b) Electrical resistivity of $SmNiC_2$ plotted on a semi-logarithmic scale near the ferromagnetic transition temperature T_c for 1 bar, 1.47, 2.72, 3.22, 3.70, 3.86, and 5.5 GPa from the tail to the head of the arrow. T_{M1} is assigned to a pressure-induced phase transition for $P > 2.18$ GPa. (c) Thermal hysteresis of ρ selectively shown for 1.47, 2.18, 2.72, and 3.22 GPa. (d) Low-temperature electrical resistivity of $SmNiC_2$ as a function of temperature plotted to demonstrate contrasting behavior across 3.8 GPa. T_{M2} and T_{M3} describe two emergent phase transitions for $P > 3.8$ GPa. Applied pressure for each data set is indicated in units of GPa.

indicating that the CDW gap opening is responsible for the charge carrier depletion and, thus, the increase in $\Delta\rho_{max}$. We note that there is a deviation from linearity at the highest pressure 5.5 GPa, which may be intrinsic and merits additional study at pressures higher than 5.5 GPa.

Thermal diffuse scattering observed by x-ray scattering measurements at ambient pressure indicates a critical phonon softening at two characteristic wavevectors of $q_1 = (0.5, 0.52, 0)$ and $q_2 = (0.5, 0.5, 0.5)$ (ref. 6). Only q_1 evolves into a CDW phase, while q_2 remains diffusive. A change in the Fermi surface can be incurred by applied pressure because of anisotropic elastic moduli. A slight suppression of T_{CDW} at low pressures manifests a weakening of the Fermi surface nesting along q_1, which opens the possibility for a new competing phase. Indeed, an additional inflection in the resistivity occurs at 68.5 K and 1.47 GPa (see Fig. 2a). Considering that there already exists lattice softening along the q_2 wavevector, the new feature may correspond to a CDW gap opening along that direction. As shown in Fig. 3a, the CDW2 transition temperature T_{CDW2} increases with pressure, reaches a maximum near 2.18 GPa, and is completely suppressed above 3.86 GPa. Here the transition temperature T_{CDW2} was determined from the point of inflection. The optimal pressure for CDW2 (≈ 2.18 GPa) coincides with the critical pressure where the original T_{CDW} starts to increase sharply, underlying that the Fermi surface topology is important to the multiple CDW phases of $SmNiC_2$.

Figure 3b shows the resistivity of $SmNiC_2$ under pressure. The first-order ferromagnetic transition temperature T_c, below which Sm moments with 0.32 μ_B are aligned parallel to the a-axis,[4] is gradually suppressed with pressure. At pressures higher than 2.18 GPa, a plateau appears in the FM transition region, indicating that the FM ground state is accessed through an intermediate phase. The initial drop in ρ is assigned as T_{M1}, while the second drop at a lower temperature as T_c because the resistivity value approaches that of ambient pressure. These results suggest that the FM transition temperature decreases continuously, but the intermediate phase observed at a higher transition temperature T_{M1} shows a dome shape with maximal value near 4.28 GPa (see Fig. 4a). Similar to $Er_5Ir_4Si_{10}$, where a CDW and antiferromagnetism coexists,[17] it is likely that the T_{M1} and CDW phases of $SmNiC_2$ coexist for $T_c \leq T \leq T_{M1}$, while the CDW disappears below T_c. Commensurate with the appearance of the intermediate $M1$ phase, as shown in Fig. 3c, thermal hysteresis in ρ for the FM transition (or the lower phase transition) is not evident within the limit of the resistivity measurements, indicating a second order or a weakly first order nature for pressures above 2.18 GPa.

The low-temperature resistivity of $SmNiC_2$ is magnified in Fig. 3d, which reveals contrasting behaviors across 3.8 GPa, a projected critical pressure for a FM quantum phase transition: ρ is sharply reduced below T_c for $P < 3.8$ GPa and is enhanced below a characteristic temperature T_{M2} for $P > 3.8$ GPa, suggesting a gap opening on the Fermi surface. With increasing pressure, T_{M2} decreases and is suppressed below 1.2 K at 4.7 GPa. A new low-T phase appears at 4.7 GPa and 3.0 K, whose transition temperature T_{M3} increases with pressure. Singular quantum fluctuations in the vicinity of a projected quantum critical point (QCP) have been proposed as a route to novel quantum phases, where the novel phase essentially hides the presence of a QCP.[13,14] The successive appearance of M2 and M3 phases that intercepts the FM phase may be associated with the abundant FM fluctuations near 3.8 GPa. Figure 4 summarizes the temperature-pressure phase diagram of $SmNiC_2$ and the isothermal electrical resistivity values at 1.2 K that

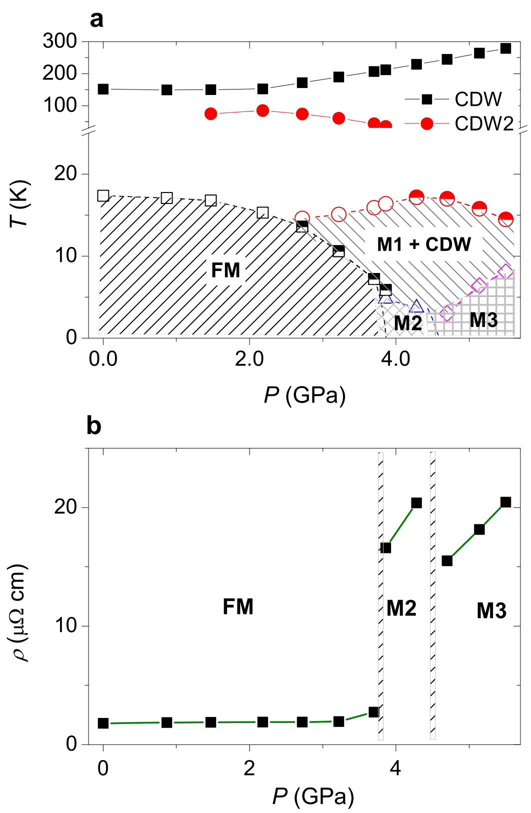

FIG. 4: (Color online) (a) Phase transition temperatures plotted against pressure. CDW phase transitions T_{CDW} (solid squares) and T_{CDW2} (solid circles) occur at high temperatures, while the FM phase transition T_c (open squares) at low temperatures is intercepted by new phases T_{M2} (open triangles) and T_{M3} (open diamonds). Half-filled squares (T_c) for $P > 2.14$ GPa and half-filled circles (T_{M1}) for $P > 4.28$ GPa represent second order or weakly first order nature of the phase transitions. (b) Resistivity of $SmNiC_2$ at 1.2 K is plotted as a function of pressure. The discontinuities in ρ observed around 3.8 and 4.5 GPa reflect magnetic quantum phase transitions from FM to M2 and to M3, successively.

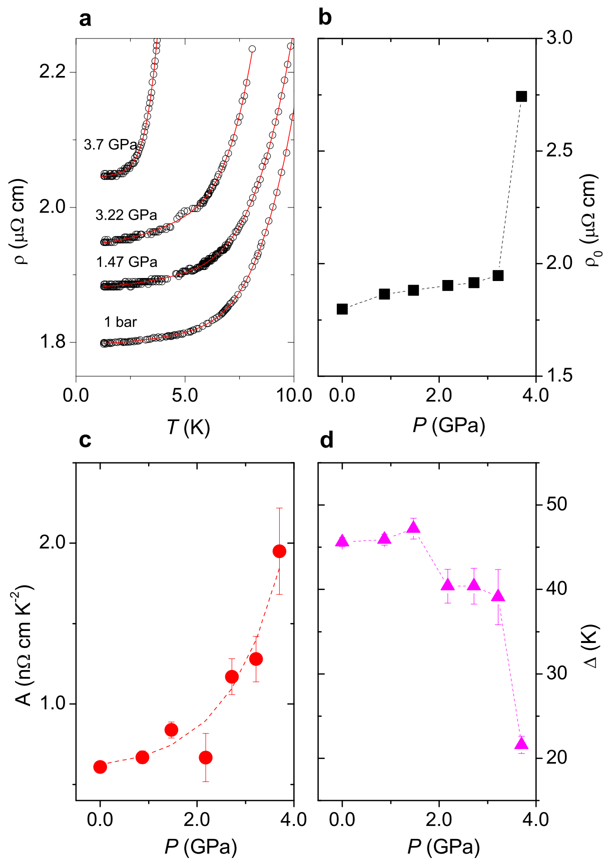

FIG. 5: (Color online) (a) Temperature dependence of the electrical resistivity of $SmNiC_2$ at 1 bar, 1.47, 3.22, and 3.7 GPa. Solid lines are least-squares fits of data to $\rho = \rho_0 + AT^2 + C_m T\Delta(1+2T/\Delta)\exp(-\Delta/T)$, where the residual resistivity ρ_0, the T^2 coefficient A, and the magnon gap Δ are obtained from the best fits and plotted as a function of pressure in (b), (c), and (d), respectively. Error bars shown in (c) and (d) are standard deviation from the least-squares fit. The symbols in (b) are larger than the error bars.

reflect the evolution of the magnetic ground states as a function of pressure.

Figure 5a representatively shows the low-T resistivity of $SmNiC_2$ within the FM phase for pressures below 3.8 GPa. For clarity, data at 3.7 GPa are rigidly shifted downward by $-0.7\mu\Omega$·cm. In order to explain the temperature dependence of the resistivity below T_c, we use the following form that is often applied to a non-cubic ferromagnetic material:[15,16] $\rho = \rho_0 + AT^2 + C_m T\Delta(1 + 2T/\Delta)e^{-\Delta/T}$, where the first and second terms are from impurity potential and electron-electron scattering, respectively. Scattering from magnons is represented by the third term, where C_m is a constant and Δ is the magnon gap amplitude. Solid lines are from a least-squares fit of the above formula and pressure evolution of the fitting parameters ρ_0, A, and Δ is plotted in Fig. 5b, 5c, and 5d, respectively. The residual resistivity ρ_0 gradually increases from 1.798 $\mu\Omega$·cm at 1 bar to 1.947 $\mu\Omega$·cm at 3.22 GPa, then sharply increases to 2.743 $\mu\Omega$·cm at 3.7 GPa. The T^2 coefficient A exponentially increases from 0.608 $n\Omega$·cm·K^{-2} at 1 bar to 1.95 $n\Omega$·cm·K^{-2} at 3.7 GPa (dashed line in Fig. 4c), suggesting an enhancement of the effective mass of $SmNiC_2$. In contrast, the magnon gap Δ that characterizes the FM state decreases with pressure. The enhancement of ρ_0 and A and suppression of the magnon gap Δ near 3.8 GPa underscores the possibility of a hidden FM QCP near 3.8 GPa.

To summarize, we have established a global phase diagram of $SmNiC_2$ by measuring electrical resistivity under pressure up to 5.5 GPa. The CDW transition temperature T_{CDW} initially decreases with pressure, reaches a minimum near 1.47 GPa, then increases sharply to 279.3 K at 5.5 GPa. An additional CDW phase appears within the original CDW phase at 1.47 GPa where T_{CDW} reaches a minimum, manifesting that nesting of the Fermi surface is important to formation of the CDWs. The first-order FM phase transition temperature T_c is grad-

ually suppressed with pressure, but bifurcates into the upper $M1$ and the lower FM phases above 2.18 GPa, where the lower FM transition changes to a second order or a weakly first order nature. The low-temperature resistivity was analyzed in terms of a Landau-Fermi liquid T^2 dependence and magnon scattering in the FM phase. The residual resistivity and the T^2 coefficient A increase with increasing pressure, while the magnon gap is almost constant up to 3.2 GPa and is sharply suppressed at 3.7 GPa, suggesting a hidden FM quantum critical point near 3.8 GPa.

This work was supported by NRF grant funded by the Korea government (MEST) (No. 2011-0021645, & 220-2011-1-C00014). Work at Los Alamos was performed under the auspices of the U. S. Department of Energy/Office of Science and supported in part by the Los Alamos LDRD program. VAS is supported in part from Russian Foundation for Basic Research (RFBR grant 12-02-00376). YSK acknowledges support from NRF grant funded by MEST (No. 2012K1A4A3053565). TP thanks J. Han and J. Shim for useful discussion.

---

[1] G. Grüner, Density Waves in Solids (Frontiers in Physics; v. **89** (1994))

[2] E. Morosan et al., Nat. Phys. **2**, 544-550 (2006).

[3] S. L. Bud'ko, P. C. Canfield, E. Morosan, R. J. Cava, and G. M. Schmiedeshoff, J. Phys.: Condens. Matter **19**, 176230 (2007).

[4] H. Onodera, Y. Kshikawa, M. Kosaka, M. Ohashi, H. Yamauchi, Y. Yamaguchi, J. Magn. Magn. Mater. **182**, 161 (1998).

[5] M. Murase, A. Tobo, H. Onodera, Y. Hirano, T. Hosaka, S. Shimomura, N. Wakabayashi, J. Phys. Soc. Jpn. **73**, 2790 (2004).

[6] S. Shimomura, C. Hayashi, G. Asaka, N. Wakabayashi, M. Mizumaki, H. Onodera, Phy. Rev. Lett. **102**, 076404 (2009)

[7] J. Laverock, T. D. Haynes, C. Ulfeld, S. B. Dugdale, Phys. Rev. B. **80**, 125111 (2009)

[8] J. Kim et al., (unpublished)

[9] J. H. Kim, J.-S. Rhyee, and Y. S. Kwon, Phys. Rev. B **86**, 235101 (2012)

[10] A. Eiling and J. S. Schilling J. Phys. F: Met. Phys. **11**, 623 (1981)

[11] A. E. Petrova, V. A. Sidorov, and S. M. Stishov, Physica B **359**, 1463 (2005).

[12] K. Kadowaki and S. B. Woods, Solid State Commun. **58**, 507 (1986).

[13] P. Coleman and A. J. Schofield, Nature **433**, 226 (2005).

[14] T. Park et al., Nature **440**, 65 (2006).

[15] N. H. Andersen and H. Smith, Phys. Rev. B **19**, 384 (1979).

[16] T. Fukuhara, R. Yamagata, L. Li, K. Nishimura, and K. Maezawa, J. Phys. Soc. Jpn. **78**, 034723 (2009).

[17] F. Galli et al., J. Phys.: Condens. Matter **14**, 5067 (2002).